Nonlinear Dyn (2018) 91:525–538
https://doi.org/10.1007/s11071-017-3887-1

ORIGINAL PAPER

Guaranteeing prescribed output tracking performance for air-breathing hypersonic vehicles via non-affine back-stepping control design

Xiangwei Bu

Received: 1 February 2017 / Accepted: 17 October 2017 / Published online: 30 October 2017

Abstract This study develops a novel back-stepping controller with prescribed performance for air-breathing hypersonic vehicles (AHVs) utilizing non-affine models. For the velocity dynamics, a non-affine control law is addressed to achieve prescribed tracking performance. The altitude subsystem is rewritten as a strict feedback formulation to facilitate the back-stepping control system design via a model transformation approach. At each step of back-stepping design, performance functions are constructed to force tracking errors to fall within prescribed boundaries, based on which desired transient performance and steady-state performance are guaranteed for both velocity and altitude control subsystems. Furthermore, the exploited controllers are accurate model independent, which guarantees control laws with satisfactory robustness against unknown uncertainties. Meanwhile, the proposed control scheme can cope with unknown control gains. By the Lyapunov stability theory, the stability of the closed-loop control system is confirmed. Finally, numerical simulations are given for an AHV to validate the effectiveness of the proposed control approach.

Keywords Air-breathing hypersonic vehicles · Prescribed performance · Non-affine control · Back-stepping · Unknown control gains

X. Bu (✉)
Air and Missile Defense College, Air Force Engineering University, Xi’an 710051, China
e-mail: buxiangwei1987@126.com

List of symbols

m	Vehicle mass
$\bar{\rho}$	Density of air
$\bar{q}$	Dynamic pressure
S	Reference area
h	Altitude
V	Velocity
γ	Flight-path angle
θ	Pitch angle
α	Angle of attack ($\alpha = \theta - \gamma$)
Q	Pitch rate
T	Thrust
D	Drag
L	Lift
M	Pitching moment
I_{yy}	Moment of inertia
$\bar{c}$	Aerodynamic chord
z_{T}	Thrust moment arm
Φ	Fuel equivalence ratio
δ_{e}	Elevator angular deflection
N_i	ith generalized force
$N_i^{\alpha_j}$	jth order contribution of α toN_i
N_i^0	Constant term inN_i
$N_2^{\delta_{\mathrm{e}}}$	Contribution of δ_{e} toN_2
$\beta_i\,(h, \bar{q})$	ith trust fit parameter
η_i	ith generalized elastic coordinate
ζ_i	Damping ratio for elastic mode η_i
ω_i	Natural frequency for elastic modeη_i
$C_D^{\alpha^i}$	ith order coefficient of α in D

$C_D^{\delta_e^i}$	ith order coefficient of δ_e in D
C_D^0	Constant coefficient in D
$C_L^{\alpha^i}$	ith order coefficient of α in L
$C_L^{\delta_e}$	Coefficient of δ_e contribution in L
C_L^0	Constant coefficient in L
$C_{M,\alpha}^{\alpha^i}$	ith order coefficient of α in M
$C_{M,\alpha}^0$	Constant coefficient in M
$C_T^{\alpha^i}$	ith order coefficient of α in T
C_T^0	Constant coefficient in T
h_0	Nominal altitude for air density approximation
$\bar{\rho}_0$	Air density at the altitudeh_0
$\tilde{\psi}_i$	Constrained beam coupling constant for η_i
c_e	Coefficient of $\delta_e$in M
$1/h_s$	Air density decay rate

1 Introduction

As a strategic near-space weapon, air-breathing hypersonic vehicles (AHVs) have seen significant developments in the past decade. Flight control design for AHVs is a challenging and meaningful research area since control systems should deal with system uncertainties, complicated couplings and model nonlinearities [1,2]. Thereby, the control gains usually are completely unknown due to system uncertainties, which results in a problem of unknown control direction [3,4]. In particular, traditional affine control methodologies are inadequate to handle such vehicles whose motion models presenting non-affine formulations. In addition, special requirements of transient performance are also needed for AHV's control systems owing to the maneuver at hypersonic speeds [5–7].

It is well known that devising efficient control approaches for AHVs is very important to complete multiple flight tasks over a wide range of flight envelopes. But varying flight environments, unknown external disturbances, and unavoidable modeling uncertainties make robust flight control design for AHVs a challenging task [8,9]. By addressing a robust tracking issue of AHVs subject to uncertainties and disturbances, an inaccuracy model-based asymptotic tracking controller is exploited based on an affine model of AHVs without using high-order time derivatives of vehicle states [10]. To weaken the undesired high-frequency chattering that may stimulate vehicle's flexible modes, a high-order sliding mode control design is presented for AHVs to provide robust tracking of reference trajectories, while avoiding traditional robust controllers' conservatism [1]. Furthermore, a terminal sliding mode control method is investigated for AHVs to achieve fast tracking of velocity and altitude commands in the presence of parametric uncertainties and unknown disturbances [11]. For an AHV with multiple disturbances, a hybrid control frame incorporating fuzzy approximation and disturbance observer is studied to reject multiple source disturbances, which guarantees the addressed controller with better practicality than the ones that only considers single type of disturbance [12]. By employing neural networks to estimate unknown dynamics, a low computational controller is developed for a constrained AHV, and simulation results prove the tracking performance of that strategy despite of uncertainties, disturbances, and control input constraints [13,14]. In [2], an active disturbance rejection control strategy is proposed for AHVs' tracking system, and extended state observers are constructed to estimate uncertainties for the sake of further enhancing the controller's robustness.

It has been proved that the altitude dynamics of AHVs is easy to be rewritten as a strict feedback formulation, which makes the recursive back-stepping design realizable [15–17]. On the basis of a newly designed nonlinear disturbance observer, a robust back-stepping control scheme is developed to steer velocity and altitude to track their reference commands, and meanwhile the problem of "explosion of terms" caused by back-stepping design is handled by a tracking differentiator [18]. The control approach exploited in [19] is to combine back-stepping with sliding mode control such that the addressed controller for AHVs with mismatched uncertainties can provide robust tracking of reference trajectories. Owing to the excellent capability of nonlinearity approximation, neural networks are incorporated with back-stepping design procedure, based on which an adaptive nonlinear controller is devised for AHVs [20]. Though the tracking performance and robustness of that scheme are validated by numerical simulations in the presence of system uncertainties and external disturbances, too many neural networks and online learning parameters are required to guarantee the robustness and convergence, which yields high computational load and results in certain control time delay. For this reason, great efforts are made to reduce the required neural networks via a model transformation [14,18,21,22] and also to decrease the utilized online learning parameters based on advanced algorithms [22–24].

Though excellent tracking performance can be achieved by the above-mentioned control methodologies, there are still some shortcomings to these approaches [1,8–24]. A fatal one is that these controllers are devised using simplified affine models, which harms their application validity in practice since AHVs' motion models are completely non-affine [25,26]. Another is that it is difficult for these control methods to guarantee prescribed output tracking performance especially transient performance for AHVs' hypersonic maneuver. In this paper, we propose a new tracking controller with prescribed performance for AHVs based on non-affine models using the back-stepping design procedure, capable of guaranteeing prescribed performance for tracking errors. The special contributions are summarized as follows.

1. The addressed controller directly stems from a non-affine model of AHVs, which avoids inappropriate model simplifications under rigorous assumptions and guarantees controllers with practicality.
2. Prescribed output tracking quality is achieved for AHVs via prescribed performance control.
3. The presented control approach is independent on accurate vehicle models and function estimations. Thus its disturbance rejection ability is fine and the computational cost is low.

The rest of this study is outlined as follows. The motion model of AHVs is formulated in Sect. 2, and the preliminary knowledge of prescribed performance is briefly explained in Sect. 3. In Sect. 4, prescribed performance back-stepping controllers are devised and the convergence of closed-loop control system is proved. Simulation results are shown in Sect. 5, and finally conclusions are presented in Sect. 6.

2 Problem formulation

2.1 Vehicle model

The longitudinal motion model considered in this paper is formulated as [25,26]

$$\dot{V} = T\cos(\theta-\gamma)/m - D/m - g\sin\gamma \tag{1}$$

$$\dot{h} = V\sin\gamma \tag{2}$$

$$\dot{\gamma} = L/(mV) + T\sin(\theta-\gamma)/(mV) - g\cos\gamma \tag{3}$$

$$\dot{\theta} = Q \tag{4}$$

$$\dot{Q} = \left(M + \tilde{\psi}_1\ddot{\eta}_1 + \tilde{\psi}_2\ddot{\eta}_2\right)/I_{yy} \tag{5}$$

$$k_1\ddot{\eta}_1 = -2\zeta_1\omega_1\dot{\eta}_1 - \omega_1^2\eta_1 + N_1 - \tilde{\psi}_1 M/I_{yy} - \tilde{\psi}_1\tilde{\psi}_2\ddot{\eta}_2/I_{yy} \tag{6}$$

$$k_2\ddot{\eta}_2 = -2\zeta_2\omega_2\dot{\eta}_2 - \omega_2^2\eta_2 + N_2 - \tilde{\psi}_2 M/I_{yy} - \tilde{\psi}_2\tilde{\psi}_1\ddot{\eta}_1/I_{yy}. \tag{7}$$

The above vehicle model consists of five rigid body states (velocity V, altitude h, flight-path angle γ, pitch angle θ, and pitch rate Q) and two flexible states (η_1 and η_2). The attack angle $\alpha = \theta - \gamma$. T, D, L, M, N_1 and N_2 denote thrust force, drag force, lift force, pitching moment, the first generalized force, and the second generalized force, respectively. Their details are as follows [26]

$$\begin{aligned}
T &\approx \beta_1(h,\bar{q})\Phi\alpha^3 + \beta_2(h,\bar{q})\alpha^3 + \beta_3(h,\bar{q})\Phi\alpha^2 \\
&\quad + \beta_4(h,\bar{q})\alpha^2 \\
&\quad + \beta_5(h,\bar{q})\Phi\alpha + \beta_6(h,\bar{q})\alpha + \beta_7(h,\bar{q})\Phi \\
&\quad + \beta_8(h,\bar{q}), \\
D &\approx \bar{q}SC_D^{\alpha^2}\alpha^2 + \bar{q}SC_D^{\alpha}\alpha + \bar{q}SC_D^{\delta_e^2}\delta_e^2 \\
&\quad + \bar{q}SC_D^{\delta_e}\delta_e + \bar{q}SC_D^0, \\
M &\approx z_T T + \bar{q}S\bar{c}C_{M,\alpha}^{\alpha^2}\alpha^2 + \bar{q}S\bar{c}C_{M,\alpha}^{\alpha}\alpha + \bar{q}S\bar{c}C_{M,\alpha}^0 \\
&\quad + \bar{q}S\bar{c}c_e\delta_e, \\
L &\approx \bar{q}SC_L^{\alpha}\alpha + \bar{q}SC_L^{\delta_e}\delta_e + \bar{q}SC_L^0, \\
N_1 &= N_1^{\alpha^2}\alpha^2 + N_1^{\alpha}\alpha + N_1^0, \\
N_2 &= N_2^{\alpha^2}\alpha^2 + N_2^{\alpha}\alpha + N_2^{\delta_e}\delta_e + N_2^0, \quad \bar{q} = \bar{\rho}V^2/2, \\
\bar{\rho} &= \bar{\rho}_0\exp(-(h-h_0)/h_s),
\end{aligned}$$

where fuel equivalence ratio Φ and elevator angular deflection δ_e are the control inputs, and they occur implicitly in Eqs. (1)–(7). For more detailed definitions of other parameters and coefficients, the reader could refer to [25,26].

Remark 1 Traditionally, only the rigid body states are measured and used for control designs, while the flexible states are treated as system uncertainties that are coped with by the controller's robustness [14–16].

2.2 Control objective

The control goal sought is to devise non-affine prescribed performance controllers Φ and δ_e via back-stepping for AHVs such that velocity V and altitude h track their reference commands V_{ref} and h_{ref} in the presence of parametric uncertainties. Meanwhile, all closed-loop signals are bounded, and the transient property's tracking performance and the steady-state error are characterized by performance functions.

3 Prescribed performance

By prescribed performance, we mean that the tracking error e evolves strictly within predefined decaying bounds as follows:

$$-\delta\rho(t) < e < \bar{\delta}\rho(t), \tag{8}$$

where the performance function $\rho(t) = (\rho_0 - \rho_\infty) e^{-lt} + \rho_\infty > 0$ is bounded and strictly positive decreasing with the property $\rho_\infty \le \rho(t) \le \rho_0$; $\rho_0 > \rho_\infty > 0$, $l > 0$, $0 < \bar{\delta} < 1$, $0 < \delta < 1$ are design parameters.

If e remains within the adjustable neighborhood of (8), the maximum overshoot of e is prescribed less than $\max\left\{\bar{\delta}\rho_0, \delta\rho_0\right\}$, and the steady value $e(\infty)$ is no more than $\max\left\{\bar{\delta}\rho_\infty, \delta\rho_\infty\right\}$. Thus, both transient performance and steady-state performance of e are guaranteed by choosing appropriate design parameters for (8).

Noting that it is hard to directly design controllers using inequality constraint (8), a transformed function $\Psi\left(\varepsilon(t)\right) = \frac{\bar{\delta}e^{\varepsilon(t)} - \delta e^{-\varepsilon(t)}}{e^{\varepsilon(t)} + e^{-\varepsilon(t)}}$ is applied to convert (8) into the following formulation.

$$e = \Psi\left(\varepsilon(t)\right)\rho(t), \tag{9}$$

where $\varepsilon(t)$ is a transformed error.

Since $\lim_{\varepsilon(t)\to+\infty} \Psi\left(\varepsilon(t)\right) = \bar{\delta}$ and $\lim_{\varepsilon(t)\to-\infty} \Psi\left(\varepsilon(t)\right) = -\delta$, (9) is equivalent to (8). Furthermore, $\Psi\left(\varepsilon(t)\right) \in \left(-\delta, \bar{\delta}\right)$ is bounded and strictly increasing.

From (9), we have

$$\varepsilon(t) = \Psi^{-1}\left(\varepsilon(t)\right) = \frac{1}{2}\ln\left(\frac{e/\rho(t) + \delta}{\bar{\delta} - e/\rho(t)}\right). \tag{10}$$

$\dot{\varepsilon}(t)$ is derived as

$$\dot{\varepsilon}(t) = r\left[\dot{e} - e\frac{\dot{\rho}(t)}{\rho(t)}\right], \tag{11}$$

with

$$\begin{aligned}
\dot{\rho}(t) &= -l\left(\rho_0 - \rho_\infty\right)e^{-lt} \in \left[-l\left(\rho_0 - \rho_\infty\right), 0\right], \\
r &= \frac{1}{2\rho(t)}\left[\frac{1}{e/\rho(t) + \delta} - \frac{1}{e/\rho(t) - \bar{\delta}}\right] \\
&= \frac{1}{2\rho(t)}\left[\frac{1}{\Psi\left(\varepsilon(t)\right)\rho(t)/\rho(t) + \delta}\right. \\
&\quad \left. - \frac{1}{\Psi\left(\varepsilon(t)\right)\rho(t)/\rho(t) - \bar{\delta}}\right] \\
&= \frac{1}{2\rho(t)}\left[\frac{1}{\Psi\left(\varepsilon(t)\right) + \delta} - \frac{1}{\Psi\left(\varepsilon(t)\right) - \bar{\delta}}\right].
\end{aligned}$$

Noticing the fact that $0 < \rho_\infty \le \rho(t) \le \rho_0$ and $\Psi\left(\varepsilon(t)\right) \in \left(-\delta, \bar{\delta}\right)$, r is bounded and satisfies $r \ge \frac{1}{2\rho_0}\left(\frac{1}{\delta} + \frac{1}{\bar{\delta}}\right) > 0$.

4 Controller design

Based on the analyses of [22,23], we decompose the motion model of AHVs into the velocity subsystem (i.e., Eq. (1)) and the altitude subsystem (i.e., Eqs. (2)–(5)) for the simplicity of control design.

4.1 Velocity controller design

According to the timescale principle [3], the velocity is slower dynamics compared with the altitude and attitude angles. When velocity varies, the altitude and attitude angles are considered to reach their steady constants. Thus, the velocity subsystem can be expressed as the following non-affine formulation.

$$\begin{cases} \dot{V} = \varphi_V(V, \Phi) \\ u_V = \Phi \\ y_V = V \end{cases} \tag{12}$$

where $\varphi_V(V, \Phi)$ is a continuous unknown function, u_V and y_V are the control input and output of velocity subsystem, respectively.

By mean value theorem [27], (12) further becomes

$$\begin{cases} \dot{V} = \beta_{V1}(V) + \beta_{V2}(V)\Phi \\ u_V = \Phi \\ y_V = V \end{cases} \tag{13}$$

with $\beta_{V2}(V) = \frac{\partial\varphi_V(V, \Phi_*)}{\partial\Phi_*} \ne 0$, $\Phi_* \in (0, \Phi)$.

Remark 2 $\beta_{V2}(V) \neq 0$ is the controllability condition of (13). There is no need of priori knowledge about sign of $\beta_{V2}(V)$ that may not be easily obtained in practice.

Assumption 1 [28] The reference command V_{ref} and its time derivative $\dot{V}_{\text{ref}}$ are bounded. That is, there exist positive constants $\bar{V}_{\text{ref}}$ and $\bar{\dot{V}}_{\text{ref}}$ such that $|V_{\text{ref}}| \leq \bar{V}_{\text{ref}}$ and $\left|\dot{V}_{\text{ref}}\right| \leq \bar{\dot{V}}_{\text{ref}}$.

Define velocity tracking error e_V

$$e_V = V - V_{\text{ref}} \tag{14}$$

Employ a performance function $\rho_V(t) = \left(\rho_{V0} - \rho_{V\infty}\right)e^{-l_V t} + \rho_{V\infty}$ to constrain e_V

$$-\delta_V \rho_V(t) < e_V < \bar{\delta}_V \rho_V(t) \tag{15}$$

where $\rho_{V0} > 0$, $\rho_{V\infty} > 0$, $l_V > 0$, $0 < \delta_V < 1$, $0 < \bar{\delta}_V < 1$ are design parameters and satisfy $\rho_{V0} > \rho_{V\infty}$, $-\delta_V \rho_{V0} < e_V(0) < \bar{\delta}_V \rho_{V0}$, $\rho_{V\infty} \leq \rho_V(t) \leq \rho_{V0}$.

We transform (15) as

$$e_V = \Psi_V\left(\varepsilon_V(t)\right)\rho_V(t) \tag{16}$$

where $\Psi_V\left(\varepsilon_V(t)\right) = \frac{\bar{\delta}_V e^{\varepsilon_V(t)} - \delta_V e^{-\varepsilon_V(t)}}{e^{\varepsilon_V(t)} + e^{-\varepsilon_V(t)}} \in \left(-\delta_V, \bar{\delta}_V\right)$ is a transformed function, $\varepsilon_V(t)$ is a transformed error, and its formulation is

$$\varepsilon_V(t) = \Psi_V^{-1}\left(\varepsilon_V(t)\right) = \frac{1}{2}\ln\left(\frac{e_V/\rho_V(t) + \delta_V}{\bar{\delta}_V - e_V/\rho_V(t)}\right). \tag{17}$$

Taking time derivative along (17) leads to

$$\begin{aligned}\dot{\varepsilon}_V(t) &= r_V\left[\dot{e}_V - e_V\frac{\dot{\rho}_V(t)}{\rho_V(t)}\right] \\ &= r_V\left[\beta_{V1}(V) + \beta_{V2}(V)\Phi - \dot{V}_{\text{ref}} - e_V\frac{\dot{\rho}_V(t)}{\rho_V(t)}\right]\end{aligned} \tag{18}$$

with $r_V = \frac{1}{2\rho_V(t)}\left[\frac{1}{e_V/\rho_V(t)+\delta_V} - \frac{1}{e_V/\rho_V(t)-\bar{\delta}_V}\right] \geq \frac{1}{2\rho_{V0}}\left(\frac{1}{\delta_V} + \frac{1}{\bar{\delta}_V}\right) > 0$, $\dot{\rho}_V(t) = -l_V\left(\rho_{V0} - \rho_{V\infty}\right)e^{-l_V t} \in \left[-l_V\left(\rho_{V0} - \rho_{V\infty}\right), 0\right)$.

From the fact that $e_V = \Psi_V\left(\varepsilon_V(t)\right)\rho_V(t)$, we obtain $e_V = V - V_{\text{ref}} = \Psi_V\left(\varepsilon_V(t)\right)\rho_V(t)$, that is, $V = \Psi_V\left(\varepsilon_V(t)\right)\rho_V(t) + V_{\text{ref}}$. Then (18) becomes

$$\begin{aligned}\dot{\varepsilon}_V(t) &= r_V\left[\beta_{V1}\left(\Psi_V\left(\varepsilon_V(t)\right)\rho_V(t) + V_{\text{ref}}\right)\right. \\ &\quad + \beta_{V2}(V)\Phi - \dot{V}_{\text{ref}} \\ &\quad \left. - \Psi_V\left(\varepsilon_V(t)\right)\rho_V(t)\frac{\dot{\rho}_V(t)}{\rho_V(t)}\right] \\ &= r_V\left[\beta_{V1}\left(\Psi_V\left(\varepsilon_V(t)\right)\rho_V(t) + V_{\text{ref}}\right)\right. \\ &\quad \left. + \beta_{V2}(V)\Phi - \dot{V}_{\text{ref}} - \Psi_V\left(\varepsilon_V(t)\right)\dot{\rho}_V(t)\right].\end{aligned} \tag{19}$$

Define Lyapunov function

$$L_V = \frac{\varepsilon_V^2(t)}{2} \tag{20}$$

Invoking (19), $\dot{L}_V$ is derived as

$$\begin{aligned}\dot{L}_V &= \varepsilon_V(t)\dot{\varepsilon}_V(t) \\ &= \varepsilon_V(t)r_V\left[\beta_{V1}\left(\Psi_V\left(\varepsilon_V(t)\right)\rho_V(t)\right.\right. \\ &\quad \left. + V_{\text{ref}}\right) + \beta_{V2}(V)\Phi - \dot{V}_{\text{ref}} \\ &\quad \left. - \Psi_V\left(\varepsilon_V(t)\right)\dot{\rho}_V(t)\right] \\ &= \varepsilon_V(t)r_V\beta_{V2}(V)\Phi \\ &\quad + \varepsilon_V(t)r_V\left[\beta_{V1}\left(\Psi_V\left(\varepsilon_V(t)\right)\rho_V(t) + V_{\text{ref}}\right)\right. \\ &\quad \left. - \dot{V}_{\text{ref}} - \Psi_V\left(\varepsilon_V(t)\right)\dot{\rho}_V(t)\right].\end{aligned} \tag{21}$$

The boundedness of $\Psi_V\left(\varepsilon_V(t)\right)$, $\rho_V(t)$ and V_{ref} leads to that $\beta_{V1}\left(\Psi_V\left(\varepsilon_V(t)\right)\rho_V(t) + V_{\text{ref}}\right)$ is also bounded. Thereby, there is a positive constant $\bar{\beta}_{V1}$ such that $\left|\beta_{V1}\left(\Psi_V\left(\varepsilon_V(t)\right)\rho_V(t) + V_{\text{ref}}\right)\right| \leq \bar{\beta}_{V1}$. Then $\dot{L}_V$ becomes

$$\dot{L}_V \leq \varepsilon_V(t)r_V\beta_{V2}(V)\Phi + \left|\varepsilon_V(t)\right|r_V\Sigma_V \tag{22}$$

with $\Sigma_V = \bar{\beta}_{V1} + \bar{\dot{V}}_{\text{ref}} + \max\{\delta_V, \bar{\delta}_V\}l_V\left(\rho_{V0} - \rho_{V\infty}\right) > 0$.

The control law Φ is chosen as

$$\begin{cases}\Phi = N_V\left(\xi_V\right)\left[\kappa_{V1}\varepsilon_V(t) + \frac{\kappa_{V2}r_V\varepsilon_V(t)}{2}\right] \\ \dot{\xi}_V = \kappa_{V1}r_V\varepsilon_V^2(t) + \frac{\kappa_{V2}r_V^2\varepsilon_V^2(t)}{2}\end{cases} \tag{23}$$

where $N_V\left(\xi_V\right) = e^{\xi_V^2}\cos(\pi\xi_V/2)$ is a Nussbaum function [3,4]; $\kappa_{V1}, \kappa_{V2} > 0$ are design parameters.

Substituting Φ into (22), we get

$$\begin{aligned}\dot{L}_V &\leq \varepsilon_V(t)r_V\beta_{V2}(V)N_V\left(\xi_V\right) \\ &\quad \left[\kappa_{V1}\varepsilon_V(t) + \frac{\kappa_{V2}r_V\varepsilon_V(t)}{2}\right] + \left|\varepsilon_V(t)\right|r_V\Sigma_V.\end{aligned} \tag{24}$$

By Young's inequality, we obtain $\left|\varepsilon_V(t)\right|r_V\Sigma_V \leq \frac{\kappa_{V2}}{2}r_V^2\varepsilon_V^2(t) + \frac{\Sigma_V^2}{2\kappa_{V2}}$. Then (24) becomes

$$\begin{aligned}
\dot{L}_V &\le \varepsilon_V(t) r_V \beta_{V2}(V) N_V(\xi_V) \\
&\quad \left[\kappa_{V1}\varepsilon_V(t) + \frac{\kappa_{V2} r_V \varepsilon_V(t)}{2}\right] + \frac{\kappa_{V2}}{2} r_V^2 \varepsilon_V^2(t) + \frac{\Sigma_V^2}{2\kappa_{V2}} \\
&= \kappa_{V1}\varepsilon_V^2(t) r_V \beta_{V2}(V) N_V(\xi_V) \\
&\quad + \frac{\kappa_{V2}}{2} r_V^2 \varepsilon_V^2(t) \left[\beta_{V2}(V) N_V(\xi_V) + 1\right] \\
&\quad + \frac{\Sigma_V^2}{2\kappa_{V2}} + \kappa_{V1}\varepsilon_V^2(t) r_V - \kappa_{V1}\varepsilon_V^2(t) r_V \\
&= \kappa_{V1}\varepsilon_V^2(t) r_V \left[\beta_{V2}(V) N_V(\xi_V) + 1\right] \\
&\quad + \frac{\kappa_{V2}}{2} r_V^2 \varepsilon_V^2(t) \left[\beta_{V2}(V) N_V(\xi_V) + 1\right] \\
&\quad + \frac{\Sigma_V^2}{2\kappa_{V2}} - \kappa_{V1}\varepsilon_V^2(t) r_V \\
&= \left[\kappa_{V1}\varepsilon_V^2(t) r_V + \frac{\kappa_{V2}}{2} r_V^2 \varepsilon_V^2(t)\right] \\
&\quad \times \left[\beta_{V2}(V) N_V(\xi_V) + 1\right] + \frac{\Sigma_V^2}{2\kappa_{V2}} - \kappa_{V1}\varepsilon_V^2(t) r_V \\
&= -\kappa_{V1} r_V \varepsilon_V^2(t) + \left[\beta_{V2}(V) N_V(\xi_V) + 1\right]\dot{\xi}_V + \frac{\Sigma_V^2}{2\kappa_{V2}} \\
&\le -\iota_V L_V + \left[\beta_{V2}(V) N_V(\xi_V) + 1\right]\dot{\xi}_V + \frac{\Sigma_V^2}{2\kappa_{V2}}
\end{aligned} \tag{25}$$

with $\iota_V = \frac{\kappa_{V1}}{\rho_{V0}}\left(\frac{1}{\delta_V} + \frac{1}{\bar{\delta}_V}\right)$.

Being multiplied by $e^{\iota_V t}$ on both sides of (25), we have

$$\begin{aligned}
\frac{\mathrm{d}}{\mathrm{d}t}\left(L_V e^{\iota_V t}\right) &\le \beta_{V2}(V) N_V(\xi_V)\dot{\xi}_V e^{\iota_V t} + \dot{\xi}_V e^{\iota_V t} \\
&\quad + \frac{\Sigma_V^2}{2\kappa_{V2}} e^{\iota_V t}.
\end{aligned} \tag{26}$$

Integrating (26) over $[0, t]$ yields

$$\begin{aligned}
0 \le L_V &\le L_V(0) + e^{-\iota_V t} \\
&\quad \times \int_0^t \beta_{V2}(V) N_V(\xi_V)\dot{\xi}_V e^{\iota_V \tau}\mathrm{d}\tau \\
&\quad + e^{-\iota_V t}\int_0^t \dot{\xi}_V e^{\iota_V \tau}\mathrm{d}\tau + \int_0^t \frac{\Sigma_V^2}{2\kappa_{V2}} e^{-\iota_V(t-\tau)}\mathrm{d}\tau
\end{aligned} \tag{27}$$

Since $\int_0^t \frac{\Sigma_V^2}{2\kappa_{V2}} e^{-\iota_V(t-\tau)}\mathrm{d}\tau = \frac{\Sigma_V^2}{2\kappa_{V2}}\frac{1}{\iota_V}\left(1 - e^{-\iota_V t}\right) \in \left[0, \frac{\Sigma_V^2}{2\kappa_{V2}}\frac{1}{\iota_V}\right)$, we know that $\int_0^t \frac{\Sigma_V^2}{2\kappa_{V2}} e^{-\iota_V(t-\tau)}\mathrm{d}\tau$ is bounded. Thus, (27) becomes

$$\begin{aligned}
0 \le L_V &\le L_{V0} + e^{-\iota_V t}\int_0^t \beta_{V2}(V) N_V(\xi_V)\dot{\xi}_V e^{\iota_V \tau}\mathrm{d}\tau \\
&\quad + e^{-\iota_V t}\int_0^t \dot{\xi}_V e^{\iota_V \tau}\mathrm{d}\tau
\end{aligned} \tag{28}$$

with $L_{V0} = L_V(0) + \frac{\Sigma_V^2}{2\kappa_{V2}}\frac{1}{\iota_V}$.

By Lemmas 1 and 2 presented in [29], we know that L_V, $e^{-\iota_V t}\int_0^t \beta_{V2}(V) N_V(\xi_V)\dot{\xi}_V e^{\iota_V \tau}\mathrm{d}\tau$ and $e^{-\iota_V t}\int_0^t \dot{\xi}_V e^{\iota_V \tau}\mathrm{d}\tau$ are bounded. Hence all the closed-loop signals are bounded, and there exists a positive constant $\bar{\varepsilon}_V$ such that $|\varepsilon_V(t)| \le \bar{\varepsilon}_V$. The inversion transformation of (17) is $\frac{e_V/\rho_V(t) + \delta_V}{\bar{\delta}_V - e_V/\rho_V(t)} = e^{2\varepsilon_V(t)}$, which yields $e_V = \frac{\bar{\delta}_V e^{2\varepsilon_V(t)} - \delta_V}{1 + e^{2\varepsilon_V(t)}}\rho_V(t)$. Finally, we have $-\delta_V \rho_V(t) < \frac{\bar{\delta}_V e^{-2\bar{\varepsilon}_V} - \delta_V}{1 + e^{-2\bar{\varepsilon}_V}}\rho_V(t) \le e_V \le \frac{\bar{\delta}_V e^{2\bar{\varepsilon}_V} - \delta_V}{1 + e^{2\bar{\varepsilon}_V}}\rho_V(t) < \bar{\delta}_V \rho_V(t)$. Thus the prescribed performance for e_V is guaranteed.

4.2 Altitude controller design

Define altitude tracking error e_h as

$$e_h = h - h_{\mathrm{ref}} \tag{29}$$

Define a performance function $\rho_h(t) = (\rho_{h0} - \rho_{h\infty})e^{-l_h t} + \rho_{h\infty} > 0$ to constrain e_h.

$$-\delta_h \rho_h(t) < e_h < \bar{\delta}_h \rho_h(t) \tag{30}$$

where $\rho_{h0} > 0$, $\rho_{h\infty} > 0$, $l_h > 0$, $0 < \delta_h < 1$, $0 < \bar{\delta}_h < 1$ are design parameters and satisfy $\rho_{h0} > \rho_{h\infty}$, $-\delta_h \rho_{h0} < e_h(0) < \bar{\delta}_h \rho_{h0}$, $\rho_{h\infty} \le \rho_h(t) \le \rho_{h0}$.

Define transformed error $\varepsilon_h(t)$ as

$$\varepsilon_h(t) = \frac{1}{2}\ln\left(\frac{e_h/\rho_h(t) + \delta_h}{\bar{\delta}_h - e_h/\rho_h(t)}\right) \tag{31}$$

The command of γ is selected as

$$\gamma_{\mathrm{d}} = \arcsin\left[\frac{-\mu_h \varepsilon_h(t) + \dot{h}_{\mathrm{ref}} + \dot{\rho}_h(t) e_h/\rho_h(t)}{V}\right] \tag{32}$$

where $\mu_h > 0$ is a design parameter, $\dot{\rho}_h(t) = -l_h(\rho_{h0} - \rho_{h\infty})e^{-l_h t}$.

If $\gamma \to \gamma_d$, the corresponding dynamics for $\varepsilon_h(t)$ is derived as

$$\mu_h \dot{\varepsilon}_h(t) + \varepsilon_h(t) = 0 \tag{33}$$

Thus $\varepsilon_h(t)$ is bounded, and there exists a positive constant $\bar{\varepsilon}_h$ such that $|\varepsilon_h(t)| \leq \bar{\varepsilon}_h$. The inversion transformation of (31) is $\frac{e_h/\rho_h(t)+\delta_h}{\bar{\delta}_h - e_h/\rho_h(t)} = e^{2\varepsilon_h(t)}$, from which we have $e_h = \frac{\bar{\delta}_h e^{2\varepsilon_h(t)} - \delta_h}{1+e^{2\varepsilon_h(t)}} \rho_h(t)$. Finally, we obtain $-\delta_h \rho_h(t) < \frac{\bar{\delta}_h e^{-2\bar{\varepsilon}_h} - \delta_h}{1+e^{-2\bar{\varepsilon}_h}} \rho_h(t) \leq e_h \leq \frac{\bar{\delta}_h e^{2\bar{\varepsilon}_h} - \delta_h}{1+e^{2\bar{\varepsilon}_h}} \rho_h(t) < \bar{\delta}_h \rho_h(t)$.

(1) Model transformation

By the timescale principle [3], attitude angles are faster dynamics compared with the velocity. When attitude angles vary, the velocity is considered to keep a constant. Thus, the altitude subsystem can be formulated as the following non-affine model.

$$\begin{cases} \dot{x}_1 = \varphi_{h1}(x_1, x_2) \\ \dot{x}_2 = x_3 \\ \dot{x}_3 = \varphi_{h3}(\mathbf{x}, \delta_\mathrm{e}) \\ u_h = \delta_\mathrm{e} \\ y_h = x_1 \end{cases} \tag{34}$$

where $\varphi_{h1}(x_1, x_2)$, $\varphi_{h3}(\mathbf{x}, \delta_\mathrm{e})$ are continuous unknown functions; u_h and y_h are the control input and output of altitude subsystem, respectively; $x_1 = \gamma$, $x_2 = \theta$, $x_3 = Q$, $\mathbf{x} = [x_1, x_2, x_3]$

Define $z_1 = x_1$, $z_2 = \dot{z}_1 = \dot{x}_1 = \varphi_{h1}(x_1, x_2)$. Then we have

$$\begin{aligned} \dot{z}_2 &= \frac{\partial \varphi_{h1}(x_1, x_2)}{\partial x_1} \dot{x}_1 + \frac{\partial \varphi_{h1}(x_1, x_2)}{\partial x_2} \dot{x}_2 \\ &= \frac{\partial \varphi_{h1}(x_1, x_2)}{\partial x_1} \varphi_{h1}(x_1, x_2) + \frac{\partial \varphi_{h1}(x_1, x_2)}{\partial x_2} x_3 \\ &\triangleq F_{h1}(\mathbf{x}) \end{aligned} \tag{35}$$

Define $z_3 = \dot{z}_2 = F_{h1}(\mathbf{x})$, and the time derivative of z_3 is

$$\begin{aligned} \dot{z}_3 &= \frac{\partial F_{h1}(\mathbf{x})}{\partial x_1} \dot{x}_1 + \frac{\partial F_{h1}(\mathbf{x})}{\partial x_2} \dot{x}_2 + \frac{\partial F_{h1}(\mathbf{x})}{\partial x_3} \dot{x}_3 \\ &= \frac{\partial F_{h1}(\mathbf{x})}{\partial x_1} \varphi_{h1}(x_1, x_2) + \frac{\partial F_{h1}(\mathbf{x})}{\partial x_2} x_3 \\ &\quad + \frac{\partial F_{h1}(\mathbf{x})}{\partial x_3} \varphi_{h3}(\mathbf{x}, \delta_\mathrm{e}) = \frac{\partial F_{h1}(\mathbf{x})}{\partial x_1} \varphi_{h1}(x_1, x_2) \\ &\quad + \frac{\partial F_{h1}(\mathbf{x})}{\partial x_2} x_3 + \frac{\partial F_{h1}(\mathbf{x})}{\partial x_3} \varphi_{h3}(\mathbf{x}, \delta_\mathrm{e}) \\ &\triangleq \Gamma_h(z_3, \delta_\mathrm{e}) \end{aligned} \tag{36}$$

Finally, we obtain the following formulation

$$\begin{cases} \dot{z}_1 = z_2 \\ \dot{z}_2 = z_3 \\ \dot{z}_3 = \Gamma_h(z_3, \delta_\mathrm{e}) \\ u_h = \delta_\mathrm{e} \\ y_h = z_1 = x_1 = \gamma \end{cases} \tag{37}$$

Utilizing mean value theorem [27], (37) becomes

$$\begin{cases} \dot{z}_1 = z_2 \\ \dot{z}_2 = z_3 \\ \dot{z}_3 = \Gamma_{h0}(z_3, 0) + \Gamma_{h1}(z_3, \delta_\mathrm{e}^*)\delta_\mathrm{e} \\ u_h = \delta_\mathrm{e} \\ y_h = z_1 = x_1 = \gamma \end{cases} \tag{38}$$

where $\Gamma_{h1}(z_3, \delta_\mathrm{e}^*) = \frac{\partial \Gamma_h(z_3, \delta_\mathrm{e}^*)}{\Gamma_h(z_3, \delta_\mathrm{e}^*)} \neq 0$, $\delta_\mathrm{e}^* \in (0, \delta_\mathrm{e})$; $\Gamma_{h0}(z_3, 0)$ is a continuous unknown function.

Remark 3 $\Gamma_{h1}(z_3, \delta_\mathrm{e}^*) \neq 0$ is the controllability condition of (38), and the strict restriction on the sign of $\Gamma_{h1}(z_3, \delta_\mathrm{e}^*)$ is released.

(2) Prescribed performance back-stepping controller design

Step 1 Define tracking error e_{h1}

$$e_{h1} = z_1 - z_{1\mathrm{d}} = z_1 - \gamma_\mathrm{d} \tag{39}$$

Define a performance function $\rho_{h1}(t) = (\rho_{h10} - \rho_{h1\infty}) e^{-l_{h1}t} + \rho_{h1\infty} > 0$ to constrain e_{h1}

$$-\delta_{h1}\rho_{h1}(t) < e_{h1} < \bar{\delta}_{h1}\rho_{h1}(t) \tag{40}$$

where $\rho_{h10} > 0$, $\rho_{h1\infty} > 0$, $l_{h1} > 0$, $0 < \delta_{h1} < 1$, $0 < \bar{\delta}_{h1} < 1$ are design parameters and satisfy $\rho_{h10} > \rho_{h1\infty}$, $-\delta_{h1}\rho_{h10} < e_{h1}(0) < \bar{\delta}_{h1}\rho_{h10}$, $\rho_{h1\infty} \leq \rho_{h1}(t) \leq \rho_{h10}$.

We convert (40) into the following formulation

$$e_{h1} = \Psi_{h1}(\varepsilon_{h1}(t))\,\rho_{h1}(t) \tag{41}$$

where $\Psi_{h1}(\varepsilon_{h1}(t)) = \frac{\bar{\delta}_{h1} e^{\varepsilon_{h1}(t)} - \delta_{h1} e^{-\varepsilon_{h1}(t)}}{e^{\varepsilon_{h1}(t)} + e^{-\varepsilon_{h1}(t)}} \in \left(-\delta_{h1}, \bar{\delta}_{h1}\right)$ is a transformed function and $\varepsilon_{h1}(t)$ is a transformed error. From (41), we get the formulation of $\varepsilon_{h1}(t)$

$$\varepsilon_{h1}(t) = \Psi_{h1}^{-1}\left(\varepsilon_{h1}(t)\right) = \frac{1}{2}\ln\left(\frac{e_{h1}/\rho_{h1}(t) + \delta_{h1}}{\bar{\delta}_{h1} - e_{h1}/\rho_{h1}(t)}\right). \tag{42}$$

Furthermore, $\dot{\varepsilon}_{h1}(t)$ is derived as

$$\begin{aligned}\dot{\varepsilon}_{h1}(t) &= r_{h1}\left[\dot{e}_{h1} - e_{h1}\frac{\dot{\rho}_{h1}(t)}{\rho_{h1}(t)}\right] \\ &= r_{h1}\left[\dot{z}_1 - \dot{\gamma}_{\mathrm{d}} - e_{h1}\frac{\dot{\rho}_{h1}(t)}{\rho_{h1}(t)}\right] \\ &= r_{h1}\left[z_2 - \dot{\gamma}_{\mathrm{d}} - e_{h1}\frac{\dot{\rho}_{h1}(t)}{\rho_{h1}(t)}\right]\end{aligned} \tag{43}$$

where $r_{h1} = \frac{1}{2\rho_{h1}(t)}\left[\frac{1}{e_{h1}/\rho_{h1}(t)+\delta_{h1}} - \frac{1}{e_{h1}/\rho_{h1}(t)-\bar{\delta}_{h1}}\right] \geq \frac{1}{2\rho_{h10}\delta_{h1}} + \frac{1}{2\rho_{h10}\bar{\delta}_{h1}} > 0$.

The virtual control law is designed as

$$z_{2\mathrm{d}} = -k_{h1}\varepsilon_{h1}(t) + \dot{\gamma}_{\mathrm{d}} + e_{h1}\frac{\dot{\rho}_{h1}(t)}{\rho_{h1}(t)} \tag{44}$$

where $k_{h1} > 0$ is a design parameter, $\dot{\rho}_{h1}(t) = -l_{h1}\left(\rho_{h10} - \rho_{h1\infty}\right)e^{-l_{h1}t}$.

Step 2 Define tracking error e_{h2}

$$e_{h2} = z_2 - z_{2\mathrm{d}} \tag{45}$$

Construct a performance function $\rho_{h2}(t) = \left(\rho_{h20} - \rho_{h2\infty}\right)e^{-l_{h2}t} + \rho_{h2\infty} > 0$ to constrain e_{h2}

$$-\delta_{h2}\rho_{h2}(t) < e_{h2} < \bar{\delta}_{h2}\rho_{h2}(t) \tag{46}$$

where $\rho_{h20} > 0$, $\rho_{h2\infty} > 0$, $l_{h2} > 0$, $0 < \delta_{h2} < 1$, $0 < \bar{\delta}_{h2} < 1$ are design parameters and satisfy $\rho_{h20} > \rho_{h2\infty}$, $-\delta_{h2}\rho_{h20} < e_{h2}(0) < \bar{\delta}_{h2}\rho_{h20}$, $\rho_{h2\infty} \leq \rho_{h2}(t) \leq \rho_{h20}$.

Equation (46) is further converted into the following formulation

$$e_{h2} = \Psi_{h2}\left(\varepsilon_{h2}(t)\right)\rho_{h2}(t) \tag{47}$$

where $\Psi_{h2}\left(\varepsilon_{h2}(t)\right) = \frac{\bar{\delta}_{h2}e^{\varepsilon_{h2}(t)} - \delta_{h2}e^{-\varepsilon_{h2}(t)}}{e^{\varepsilon_{h2}(t)} + e^{-\varepsilon_{h2}(t)}} \in \left(-\delta_{h2}, \bar{\delta}_{h2}\right)$ is a transformed function and $\varepsilon_{h2}(t)$ is a transformed error. From (47), we have

$$\varepsilon_{h2}(t) = \Psi_{h2}^{-1}\left(\varepsilon_{h2}(t)\right) = \frac{1}{2}\ln\left(\frac{e_{h2}/\rho_{h2}(t) + \delta_{h2}}{\bar{\delta}_{h2} - e_{h2}/\rho_{h2}(t)}\right). \tag{48}$$

The time derivative of $\varepsilon_{h2}(t)$ is

$$\begin{aligned}\dot{\varepsilon}_{h2}(t) &= r_{h2}\left[\dot{e}_{h2} - e_{h2}\frac{\dot{\rho}_{h2}(t)}{\rho_{h2}(t)}\right] \\ &= r_{h2}\left[\dot{z}_2 - \dot{z}_{2\mathrm{d}} - e_{h2}\frac{\dot{\rho}_{h2}(t)}{\rho_{h2}(t)}\right] \\ &= r_{h2}\left[z_3 - \dot{z}_{2\mathrm{d}} - e_{h2}\frac{\dot{\rho}_{h2}(t)}{\rho_{h2}(t)}\right]\end{aligned} \tag{49}$$

where $r_{h2} = \frac{1}{2\rho_{h2}(t)}\left[\frac{1}{e_{h2}/\rho_{h2}(t)+\delta_{h2}} - \frac{1}{e_{h2}/\rho_{h2}(t)-\bar{\delta}_{h2}}\right] \geq \frac{1}{2\rho_{h20}}\left(\frac{1}{\delta_{h2}} + \frac{1}{\bar{\delta}_{h2}}\right) > 0$.

The virtual control law is devised as

$$z_{3\mathrm{d}} = -k_{h2}\varepsilon_{h2}(t) + \dot{z}_{2\mathrm{d}} + e_{h2}\frac{\dot{\rho}_{h2}(t)}{\rho_{h2}(t)} \tag{50}$$

where $k_{h2} > 0$ is a design parameter, $\dot{\rho}_{h2}(t) = -l_{h2}\left(\rho_{h20} - \rho_{h2\infty}\right)e^{-l_{h2}t}$.

Step 3 Define tracking error e_{h3}

$$e_{h3} = z_3 - z_{3\mathrm{d}} \tag{51}$$

Devise a performance function $\rho_{h3}(t) = \left(\rho_{h30} - \rho_{h3\infty}\right)e^{-l_{h3}t} + \rho_{h3\infty} > 0$ to constrain e_{h3}

$$-\delta_{h3}\rho_{h3}(t) < e_{h3} < \bar{\delta}_{h3}\rho_{h3}(t) \tag{52}$$

with $\rho_{h30} > 0$, $\rho_{h3\infty} > 0$, $l_{h3} > 0$, $0 < \delta_{h3} < 1$, $0 < \bar{\delta}_{h3} < 1$ being design parameters and satisfying $\rho_{h30} > \rho_{h3\infty}$, $-\delta_{h3}\rho_{h30} < e_{h3}(0) < \bar{\delta}_{h3}\rho_{h30}$, $\rho_{h3\infty} \leq \rho_{h3}(t) \leq \rho_{h30}$.

We transform (52) into an equivalent formulation

$$e_{h3} = \Psi_{h3}\left(\varepsilon_{h3}(t)\right)\rho_{h3}(t) \tag{53}$$

where $\Psi_{h3}\left(\varepsilon_{h3}(t)\right) = \frac{\bar{\delta}_{h3}e^{\varepsilon_{h3}(t)} - \delta_{h3}e^{-\varepsilon_{h3}(t)}}{e^{\varepsilon_{h3}(t)} + e^{-\varepsilon_{h3}(t)}} \in \left(-\delta_{h3}, \bar{\delta}_{h3}\right)$ is a transformed function and $\varepsilon_{h3}(t)$ is a transformed error. The inversion of (53) is as follows

$$\varepsilon_{h3}(t) = \Psi_{h3}^{-1}\left(\varepsilon_{h3}(t)\right) = \frac{1}{2}\ln\left(\frac{e_{h3}/\rho_{h3}(t) + \delta_{h3}}{\bar{\delta}_{h3} - e_{h3}/\rho_{h3}(t)}\right). \tag{54}$$

$\dot{\varepsilon}_{h3}(t)$ is derived as

$$\begin{aligned}\dot{\varepsilon}_{h3}(t) &= r_{h3}\left[\dot{e}_{h3} - e_{h3}\frac{\dot{\rho}_{h3}(t)}{\rho_{h3}(t)}\right] \\ &= r_{h3}\left[\dot{z}_3 - \dot{z}_{3\mathrm{d}} - e_{h3}\frac{\dot{\rho}_{h3}(t)}{\rho_{h3}(t)}\right]\end{aligned}$$

$$
\begin{aligned}
&= r_{h3}\left[\Gamma_{h0}(z_3,0)+\Gamma_{h1}(z_3,\delta_e^*)\delta_e-\dot z_{3d}-e_{h3}\frac{\dot\rho_{h3}(t)}{\rho_{h3}(t)}\right]\\
&= r_{h3}\left[\Gamma_{h0}(z_3,0)+\Gamma_{h1}(z_3,\delta_e^*)\delta_e-\dot z_{3d}\right.\\
&\quad\left.-\ \Psi_{h3}\left(\varepsilon_{h3}(t)\right)\rho_{h3}(t)\frac{\dot\rho_{h3}(t)}{\rho_{h3}(t)}\right]\\
&= r_{h3}\left[\Gamma_{h0}(z_3,0)+\Gamma_{h1}(z_3,\delta_e^*)\delta_e-\dot z_{3d}\right.\\
&\quad\left.-\ \Psi_{h3}\left(\varepsilon_{h3}(t)\right)\dot\rho_{h3}(t)\right]
\end{aligned}\tag{55}
$$

with $r_{h3}=\frac{1}{2\rho_{h3}(t)}\left[\frac{1}{e_{h3}/\rho_{h3}(t)+\delta_{h3}}-\frac{1}{e_{h3}/\rho_{h3}(t)-\bar\delta_{h3}}\right]\geq\frac{1}{2\rho_{h30}}\left(\frac{1}{\delta_{h3}}+\frac{1}{\bar\delta_{h3}}\right)>0$.

Define Lyapunov function

$$
L_h=\frac{\varepsilon_{h1}^2(t)}{2}+\frac{\varepsilon_{h2}^2(t)}{2}+\frac{\varepsilon_{h3}^2(t)}{2}. \tag{56}
$$

Employing (43), (49) and (55), $\dot L_h$ is

$$
\begin{aligned}
\dot L_h &= \varepsilon_{h1}(t)\dot\varepsilon_{h1}(t)+\varepsilon_{h2}(t)\dot\varepsilon_{h2}(t)+\varepsilon_{h3}(t)\dot\varepsilon_{h3}(t)\\
&= \varepsilon_{h1}(t)r_{h1}\left[z_2-\dot\gamma_d-e_{h1}\frac{\dot\rho_{h1}(t)}{\rho_{h1}(t)}\right]\\
&\quad+\varepsilon_{h2}(t)r_{h2}\left[z_3-\dot z_{2d}-e_{h2}\frac{\dot\rho_{h2}(t)}{\rho_{h2}(t)}\right]\\
&\quad+\varepsilon_{h3}(t)r_{h3}\left[\Gamma_{h0}(z_3,0)+\Gamma_{h1}(z_3,\delta_e^*)\delta_e-\dot z_{3d}\right.\\
&\quad\left.-\ \Psi_{h3}\left(\varepsilon_{h3}(t)\right)\dot\rho_{h3}(t)\right]\\
&= \varepsilon_{h1}(t)r_{h1}\left[e_{h2}+z_{2d}-\dot\gamma_d-e_{h1}\frac{\dot\rho_{h1}(t)}{\rho_{h1}(t)}\right]\\
&\quad+\varepsilon_{h3}(t)r_{h3}\Gamma_{h1}(z_3,\delta_e^*)\delta_e+\varepsilon_{h3}(t)r_{h3}\\
&\quad\times\left[\Gamma_{h0}(z_3,0)-\dot z_{3d}\right.\\
&\quad\left.-\ \Psi_{h3}\left(\varepsilon_{h3}(t)\right)\dot\rho_{h3}(t)\right].
\end{aligned}\tag{57}
$$

Substituting (44) and (50) into (57) leads to

$$
\begin{aligned}
\dot L_h &= \varepsilon_{h1}(t)r_{h1}\left[e_{h2}-k_{h1}\varepsilon_{h1}(t)\right]+\varepsilon_{h2}(t)r_{h2}\\
&\quad\times\left[e_{h3}-k_{h2}\varepsilon_{h2}(t)\right]\\
&\quad+\varepsilon_{h3}(t)r_{h3}\left[\Gamma_{h0}(z_3,0)+\Gamma_{h1}(z_3,\delta_e^*)\delta_e-\dot z_{3d}\right.\\
&\quad\left.-\ \Psi_{h3}\left(\varepsilon_{h3}(t)\right)\dot\rho_{h3}(t)\right]\\
&= \varepsilon_{h1}(t)r_{h1}\left[\Psi_{h2}\left(\varepsilon_{h2}(t)\right)\rho_{h2}(t)-k_{h1}\varepsilon_{h1}(t)\right]\\
&\quad+\varepsilon_{h2}(t)r_{h2}\left[\Psi_{h3}\left(\varepsilon_{h3}(t)\right)\rho_{h3}(t)-k_{h2}\varepsilon_{h2}(t)\right]\\
&\quad+\varepsilon_{h3}(t)r_{h3}\Gamma_{h1}(z_3,\delta_e^*)\delta_e+\varepsilon_{h3}(t)r_{h3}\left[\Gamma_{h0}(z_3,0)\right.\\
&\quad\left.-\ \dot z_{3d}-\Psi_{h3}\left(\varepsilon_{h3}(t)\right)\dot\rho_{h3}(t)\right]\\
&= r_{h1}\left[\Psi_{h2}\left(\varepsilon_{h2}(t)\right)\rho_{h2}(t)\varepsilon_{h1}(t)-k_{h1}\varepsilon_{h1}^2(t)\right]\\
&\quad+r_{h2}\left[\Psi_{h3}\left(\varepsilon_{h3}(t)\right)\rho_{h3}(t)\varepsilon_{h2}(t)-k_{h2}\varepsilon_{h2}^2(t)\right]\\
&\quad+\varepsilon_{h3}(t)r_{h3}\Gamma_{h1}(z_3,\delta_e^*)\delta_e\\
&\quad+\varepsilon_{h3}(t)r_{h3}\left[\Gamma_{h0}(\Psi_{h3}\left(\varepsilon_{h3}(t)\right)\rho_{h3}(t)\right.\\
&\quad\left.+\ z_{3d},0)-\dot z_{3d}-\Psi_{h3}\left(\varepsilon_{h3}(t)\right)\dot\rho_{h3}(t)\right]
\end{aligned}\tag{58}
$$

It is easy to conclude that there exists a positive constant Σ_h such that $\left|\Gamma_{h0}(\Psi_{h3}\left(\varepsilon_{h3}(t)\right)\rho_{h3}(t)+z_{3d},0)-\dot z_{3d}-\Psi_{h3}\left(\varepsilon_{h3}(t)\right)\dot\rho_{h3}(t)\right|\leq\Sigma_h$. Furthermore, $\rho_{h2\infty}\leq\rho_{h2}(t)\leq\rho_{h20}$,

$\rho_{h3\infty}\leq\rho_{h3}(t)\leq\rho_{h30}$, $r_{h1}\geq\frac{1}{2\rho_{h10}}\left(\frac{1}{\delta_{h1}}+\frac{1}{\bar\delta_{h1}}\right)>0$,

$r_{h2}\geq\frac{1}{2\rho_{h20}}\left(\frac{1}{\delta_{h2}}+\frac{1}{\bar\delta_{h2}}\right)>0$,

$\Psi_{h2}\left(\varepsilon_{h2}(t)\right)=\frac{\bar\delta_{h2}e^{\varepsilon_{h2}(t)}-\delta_{h2}e^{-\varepsilon_{h2}(t)}}{e^{\varepsilon_{h2}(t)}+e^{-\varepsilon_{h2}(t)}}\in\left(-\delta_{h2},\bar\delta_{h2}\right)$,

$\Psi_{h3}\left(\varepsilon_{h3}(t)\right)=\frac{\bar\delta_{h3}e^{\varepsilon_{h3}(t)}-\delta_{h3}e^{-\varepsilon_{h3}(t)}}{e^{\varepsilon_{h3}(t)}+e^{-\varepsilon_{h3}(t)}}\in\left(-\delta_{h3},\bar\delta_{h3}\right)$.

Then (58) becomes

$$
\begin{aligned}
\dot L_h &\leq r_{h1}\left[\bar\delta_{h2}\rho_{h20}\left|\varepsilon_{h1}(t)\right|-k_{h1}\varepsilon_{h1}^2(t)\right]\\
&\quad+r_{h2}\left[\bar\delta_{h3}\rho_{h30}\left|\varepsilon_{h2}(t)\right|-k_{h2}\varepsilon_{h2}^2(t)\right]\\
&\quad+\varepsilon_{h3}(t)r_{h3}\Gamma_{h1}(z_3,\delta_e^*)\delta_e+\left|\varepsilon_{h3}(t)\right|r_{h3}\Sigma_h\\
&= r_{h1}\left|\varepsilon_{h1}(t)\right|\left[\bar\delta_{h2}\rho_{h20}-k_{h1}\left|\varepsilon_{h1}(t)\right|\right]\\
&\quad+r_{h2}\left|\varepsilon_{h2}(t)\right|\left[\bar\delta_{h3}\rho_{h30}-k_{h2}\left|\varepsilon_{h2}(t)\right|\right]\\
&\quad+\varepsilon_{h3}(t)r_{h3}\Gamma_{h1}(z_3,\delta_e^*)\delta_e+\left|\varepsilon_{h3}(t)\right|r_{h3}\Sigma_h.
\end{aligned}\tag{59}
$$

Finally, the actual control law δ_e is chosen as

$$
\begin{cases}
\delta_e=N_{h3}\left(\xi_{h3}\right)\left[\kappa_{h31}\varepsilon_{h3}(t)+\frac{\kappa_{h32}r_{h3}\varepsilon_{h3}(t)}{2}\right]\\
\dot\xi_{h3}=\kappa_{h31}r_{h3}\varepsilon_{h3}^2(t)+\frac{\kappa_{h32}r_{h3}^2\varepsilon_{h3}^2(t)}{2}
\end{cases}\tag{60}
$$

where $N_{h3}\left(\xi_{h3}\right)=e^{\xi_{h3}^2}\cos(\pi\xi_{h3}/2)$ is a Nussbaum function [3,4]; $\kappa_{h31},\kappa_{h32}>0$ are design parameters.

Invoking (60), (59) becomes

$$
\begin{aligned}
\dot L_h &\leq r_{h1}\left|\varepsilon_{h1}(t)\right|\left[\bar\delta_{h2}\rho_{h20}-k_{h1}\left|\varepsilon_{h1}(t)\right|\right]\\
&\quad+r_{h2}\left|\varepsilon_{h2}(t)\right|\left[\bar\delta_{h3}\rho_{h30}-k_{h2}\left|\varepsilon_{h2}(t)\right|\right]\\
&\quad+\varepsilon_{h3}(t)r_{h3}\Gamma_{h1}(z_3,\delta_e^*)N_{h3}\left(\xi_{h3}\right)\left[\kappa_{h31}\varepsilon_{h3}(t)\right.\\
&\quad\left.+\ \frac{\kappa_{h32}r_{h3}\varepsilon_{h3}(t)}{2}\right]+\left|\varepsilon_{h3}(t)\right|r_{h3}\Sigma_h.
\end{aligned}\tag{61}
$$

Based on Young's inequality, we get $\left|\varepsilon_{h3}(t)\right|r_{h3}\Sigma_V\leq\frac{\kappa_{h32}}{2}r_{h3}^2\varepsilon_{h3}^2(t)+\frac{\Sigma_h^2}{2\kappa_{h32}}$. Then (61) further becomes

$$
\begin{aligned}
\dot L_h &\leq r_{h1}\left|\varepsilon_{h1}(t)\right|\left[\bar\delta_{h2}\rho_{h20}-k_{h1}\left|\varepsilon_{h1}(t)\right|\right]\\
&\quad+r_{h2}\left|\varepsilon_{h2}(t)\right|\left[\bar\delta_{h3}\rho_{h30}-k_{h2}\left|\varepsilon_{h2}(t)\right|\right]\\
&\quad+\varepsilon_{h3}(t)r_{h3}\Gamma_{h1}(z_3,\delta_e^*)N_{h3}\left(\xi_{h3}\right)\\
&\quad\left[\kappa_{h31}\varepsilon_{h3}(t)+\frac{\kappa_{h32}r_{h3}\varepsilon_{h3}(t)}{2}\right]
\end{aligned}
$$

$$
\begin{aligned}
&+\frac{\kappa_{h32}}{2}r_{h3}^2\varepsilon_{h3}^2(t)+\frac{\Sigma_h^2}{2\kappa_{h32}}\\
&=r_{h1}\left|\varepsilon_{h1}(t)\right|\left[\bar{\delta}_{h2}\rho_{h20}-k_{h1}\left|\varepsilon_{h1}(t)\right|\right]\\
&\quad+r_{h2}\left|\varepsilon_{h2}(t)\right|\left[\bar{\delta}_{h3}\rho_{h30}-k_{h2}\left|\varepsilon_{h2}(t)\right|\right]\\
&\quad+\Gamma_{h1}(z_3,\delta_e^*)N_{h3}\left(\xi_{h3}\right)\\
&\quad\times\left[\kappa_{h31}r_{h3}\varepsilon_{h3}^2(t)+\frac{\kappa_{h32}r_{h3}^2\varepsilon_{h3}^2(t)}{2}\right]\\
&\quad+\frac{\kappa_{h32}}{2}r_{h3}^2\varepsilon_{h3}^2(t)+\frac{\Sigma_h^2}{2\kappa_{h32}}\\
&=r_{h1}\left|\varepsilon_{h1}(t)\right|\left[\bar{\delta}_{h2}\rho_{h20}-k_{h1}\left|\varepsilon_{h1}(t)\right|\right]\\
&\quad+r_{h2}\left|\varepsilon_{h2}(t)\right|\left[\bar{\delta}_{h3}\rho_{h30}-k_{h2}\left|\varepsilon_{h2}(t)\right|\right]\\
&\quad+\Gamma_{h1}(z_3,\delta_e^*)N_{h3}\left(\xi_{h3}\right)\dot{\xi}_{h3}\\
&\quad+\frac{\kappa_{h32}}{2}r_{h3}^2\varepsilon_{h3}^2(t)+\frac{\Sigma_h^2}{2\kappa_{h32}}\\
&=r_{h1}\left|\varepsilon_{h1}(t)\right|\left[\bar{\delta}_{h2}\rho_{h20}-k_{h1}\left|\varepsilon_{h1}(t)\right|\right]\\
&\quad+r_{h2}\left|\varepsilon_{h2}(t)\right|\left[\bar{\delta}_{h3}\rho_{h30}-k_{h2}\left|\varepsilon_{h2}(t)\right|\right]\\
&\quad+\Gamma_{h1}(z_3,\delta_e^*)N_{h3}\left(\xi_{h3}\right)\dot{\xi}_{h3}\\
&\quad-\kappa_{h31}r_{h3}\varepsilon_{h3}^2(t)+\kappa_{h31}r_{h3}\varepsilon_{h3}^2(t)\\
&\quad+\frac{\kappa_{h32}}{2}r_{h3}^2\varepsilon_{h3}^2(t)+\frac{\Sigma_h^2}{2\kappa_{h32}}\\
&=r_{h1}\left|\varepsilon_{h1}(t)\right|\left[\bar{\delta}_{h2}\rho_{h20}-k_{h1}\left|\varepsilon_{h1}(t)\right|\right]\\
&\quad+r_{h2}\left|\varepsilon_{h2}(t)\right|\left[\bar{\delta}_{h3}\rho_{h30}-k_{h2}\left|\varepsilon_{h2}(t)\right|\right]\\
&\quad-\kappa_{h31}r_{h3}\varepsilon_{h3}^2(t)+\Gamma_{h1}(z_3,\delta_e^*)\\
&\quad\times N_{h3}\left(\xi_{h3}\right)\dot{\xi}_{h3}+\dot{\xi}_{h3}+\frac{\Sigma_h^2}{2\kappa_{h32}}
\end{aligned}\tag{62}
$$

If $|\varepsilon_{h1}(t)|\le\bar{\delta}_{h2}\rho_{h20}/k_{h1}$ and $|\varepsilon_{h2}(t)|\le\bar{\delta}_{h3}\rho_{h30}/k_{h2}$, then $\varepsilon_{h1}(t)$ and $\varepsilon_{h2}(t)$ are bounded. Else if $|\varepsilon_{h1}(t)|>\bar{\delta}_{h2}\rho_{h20}/k_{h1}$ and $|\varepsilon_{h2}(t)|>\bar{\delta}_{h3}\rho_{h30}/k_{h2}$, we obtain $r_{h1}\left|\varepsilon_{h1}(t)\right|\left[\bar{\delta}_{h2}\rho_{h20}-k_{h1}\left|\varepsilon_{h1}(t)\right|\right]<0$ and $r_{h2}\left|\varepsilon_{h2}(t)\right|\left[\bar{\delta}_{h3}\rho_{h30}-k_{h2}\left|\varepsilon_{h2}(t)\right|\right]<0$. Moreover, we easily know that there exist adequately small constants $0<\kappa_{H1}<r_{h1}k_{h1}$ and $0<\kappa_{H2}<r_{h2}k_{h2}$ such that $r_{h1}\left|\varepsilon_{h1}(t)\right|\left[\bar{\delta}_{h2}\rho_{h20}-k_{h1}\left|\varepsilon_{h1}(t)\right|\right]+\kappa_{H1}\varepsilon_{h1}^2(t)<0$ and $r_{h2}\left|\varepsilon_{h2}(t)\right|\left[\bar{\delta}_{h3}\rho_{h30}-k_{h2}\left|\varepsilon_{h2}(t)\right|\right]+\kappa_{H2}\varepsilon_{h2}^2(t)<0$. Thus (62) becomes

$$
\begin{aligned}
\dot{L}_h&\le r_{h1}\left|\varepsilon_{h1}(t)\right|\left[\bar{\delta}_{h2}\rho_{h20}-k_{h1}\left|\varepsilon_{h1}(t)\right|\right]\\
&\quad+\kappa_{H1}\varepsilon_{h1}^2(t)-\kappa_{H1}\varepsilon_{h1}^2(t)+r_{h2}\left|\varepsilon_{h2}(t)\right|\\
&\quad\left[\bar{\delta}_{h3}\rho_{h30}-k_{h2}\left|\varepsilon_{h2}(t)\right|\right]+\kappa_{H2}\varepsilon_{h2}^2(t)-\kappa_{H2}\varepsilon_{h2}^2(t)\\
&\quad-\kappa_{h31}r_{h3}\varepsilon_{h3}^2(t)+\Gamma_{h1}(z_3,\delta_e^*)\\
&\quad\times N_{h3}\left(\xi_{h3}\right)\dot{\xi}_{h3}+\dot{\xi}_{h3}+\frac{\Sigma_h^2}{2\kappa_{h32}}\\
&\le-\kappa_{H1}\varepsilon_{h1}^2(t)-\kappa_{H2}\varepsilon_{h2}^2(t)-\kappa_{h31}r_{h3}\varepsilon_{h3}^2(t)\\
&\quad+\Gamma_{h1}(z_3,\delta_e^*)N_{h3}\left(\xi_{h3}\right)\dot{\xi}_{h3}+\dot{\xi}_{h3}+\frac{\Sigma_h^2}{2\kappa_{h32}}\\
&\le-\iota_hL_h+\Gamma_{h1}(z_3,\delta_e^*)N_{h3}\left(\xi_{h3}\right)\dot{\xi}_{h3}+\dot{\xi}_{h3}\\
&\quad+\frac{\Sigma_h^2}{2\kappa_{h32}}
\end{aligned}\tag{63}
$$

with $\iota_h=\min\left\{2\kappa_{H1},2\kappa_{H2},\frac{\kappa_{h31}}{\rho_{h30}}\left(\frac{1}{\underline{\delta}_{h3}}+\frac{1}{\bar{\delta}_{h3}}\right)\right\}$.

Being multiplied by e^{ι_ht} on both sides of (63) leads to

$$
\begin{aligned}
\frac{\mathrm{d}}{\mathrm{d}t}\left(L_he^{\iota_ht}\right)&\le\Gamma_{h1}(z_3,\delta_e^*)N_{h3}\left(\xi_{h3}\right)\dot{\xi}_{h3}e^{\iota_ht}\\
&\quad+\dot{\xi}_{h3}e^{\iota_ht}+\frac{\Sigma_h^2}{2\kappa_{h32}}e^{\iota_ht}
\end{aligned}\tag{64}
$$

Integrating (64) over $[0,t]$, we obtain

$$
\begin{aligned}
0&\le L_h\le L_h(0)+e^{-\iota_ht}\\
&\quad\times\int_0^t\Gamma_{h1}(z_3,\delta_e^*)N_{h3}\left(\xi_{h3}\right)\dot{\xi}_{h3}e^{\iota_h\tau}\mathrm{d}\tau\\
&\quad+e^{-\iota_ht}\int_0^t\dot{\xi}_{h3}e^{\iota_h\tau}\mathrm{d}\tau+\int_0^t\frac{\Sigma_h^2}{2\kappa_{h32}}e^{-\iota_h(t-\tau)}\mathrm{d}\tau
\end{aligned}\tag{65}
$$

Noticing $\int_0^t\frac{\Sigma_h^2}{2\kappa_{h32}}e^{-\iota_h(t-\tau)}\mathrm{d}\tau=\frac{\Sigma_h^2}{2\kappa_{h32}}\frac{1}{\iota_h}\left(1-e^{-\iota_ht}\right)\in\left[0,\frac{\Sigma_h^2}{2\kappa_{h32}}\frac{1}{\iota_h}\right)$, we know that $\int_0^t\frac{\Sigma_h^2}{2\kappa_{h32}}e^{-\iota_h(t-\tau)}\mathrm{d}\tau$ is bounded. Furthermore, (65) becomes

$$
\begin{aligned}
0&\le L_h\le L_{h0}+e^{-\iota_ht}\int_0^t\Gamma_{h1}(z_3,\delta_e^*)\\
&\quad\times N_{h3}\left(\xi_{h3}\right)\dot{\xi}_{h3}e^{\iota_h\tau}\mathrm{d}\tau+e^{-\iota_ht}\int_0^t\dot{\xi}_{h3}e^{\iota_h\tau}\mathrm{d}\tau
\end{aligned}\tag{66}
$$

with $L_{h0}=L_h(0)+\frac{\Sigma_h^2}{2\kappa_{h32}}\frac{1}{\iota_h}$.

Invoking Lemmas 1 and 2 presented in [29], we have that L_h, $e^{-\iota_ht}\int_0^t\Gamma_{h1}(z_3,\delta_e^*)N_{h3}\left(\xi_{h3}\right)\dot{\xi}_{h3}e^{\iota_h\tau}\mathrm{d}\tau$ and $e^{-\iota_ht}\int_0^t\dot{\xi}_{h3}e^{\iota_h\tau}\mathrm{d}\tau$ are all bounded. Thus, all the closed-loop signals are bounded. From the boundedness of $\varepsilon_i(t)$, $i=h1,h2,h3$, we know that there exist positive constant $\bar{\varepsilon}_i$, $i=h1,h2,h3$ such that $|\varepsilon_i(t)|\le\bar{\varepsilon}_i$, $i=h1,h2,h3$. Further, the inversions of $\varepsilon_i(t)$, $i=h1,h2,h3$ are $\frac{e_i/\rho_i(t)+\underline{\delta}_i}{\bar{\delta}_i-e_i/\rho_i(t)}=e^{2\varepsilon_i(t)}$, $i=h1,h2,h3$. That is, $e_i=\frac{\bar{\delta}_ie^{2\varepsilon_i(t)}-\underline{\delta}_i}{1+e^{2\varepsilon_i(t)}}\rho_i(t)$, $i=h1,h2,h3$, which leads to $-\underline{\delta}_i\rho_i(t)<\frac{\bar{\delta}_ie^{-2\bar{\varepsilon}_i}-\underline{\delta}_i}{1+e^{-2\bar{\varepsilon}_i}}\rho_i(t)\le e_i\le\frac{\bar{\delta}_ie^{2\bar{\varepsilon}_i}-\underline{\delta}_i}{1+e^{2\bar{\varepsilon}_i}}\rho_i(t)<\bar{\delta}_i\rho_i(t)$, $i=h1,h2,h3$. Obviously, the prescribed performance for e_{h1}, e_{h2} and e_{h3} is guaranteed.

The design procedure of velocity and altitude controllers is completed. The structure of the addressed control approach is presented in Fig. 1.

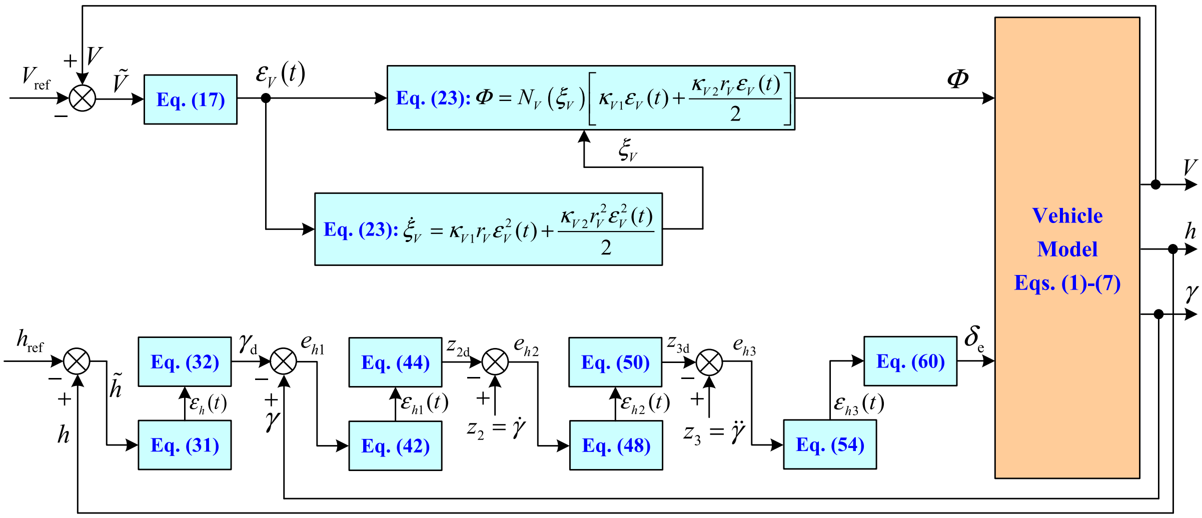

Fig. 1 The structure of the proposed control strategy

Remark 4 It is apparent that the developed control laws (23), (44), (50) and (60) do not rely on vehicle models, which guarantees the control system with satisfactory robustness against uncertainties.

Remark 5 The above analysis reveals that prescribed output tracking performance for tracking errors e_V, e_h, e_{h1}, e_{h2} and e_{h3} is achieved by selecting appropriate design parameters for (15), (30), (40), (46) and (52).

Remark 6 The addressed control laws (23), (44), (50) and (60) are designed based on non-affine models (12) and (37) only using equal transformations from (12), (37) to (13), (38), on the basis of which the proposed control methodology presents good practicality because there is no need of model simplification.

5 Simulation results

In this section, the effectiveness of presented control strategy is verified through simulation. Moreover, to show the superiority, the investigated controller is compared with a dynamic surface control-based neural control scheme proposed in [20]. The design parameters are chosen as follows: $\rho_{V0} = 10$, $\rho_{V\infty} = 1.5$, $l_V = 0.05$, $\delta_V = \bar{\delta}_V = 0.9$, $\kappa_{V1} = -15$, $\kappa_{V2} = 0.5$, $\rho_{h0} = 0.4$, $\rho_{h\infty} = 0.1$, $l_h = 0.05$, $\delta_h = \bar{\delta}_h = 0.5$, $\mu_h = 15$, $\rho_{h10} = 0.087$, $\rho_{h1\infty} = 0.026$, $l_{h1} = 0.1$, $\delta_{h1} = \bar{\delta}_{h1} = 0.5$, $k_{h1} = 0.02$, $\rho_{h20} = 0.087$, $\rho_{h2\infty} = 0.026$, $l_{h2} = 0.1$, $\delta_{h2} = \bar{\delta}_{h2} = 0.5$,

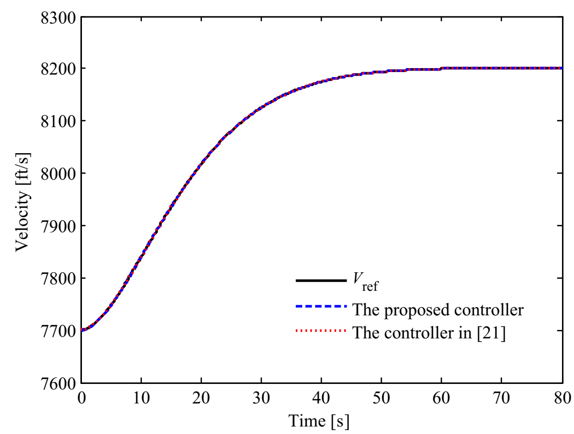

Fig. 2 Velocity tracking performance

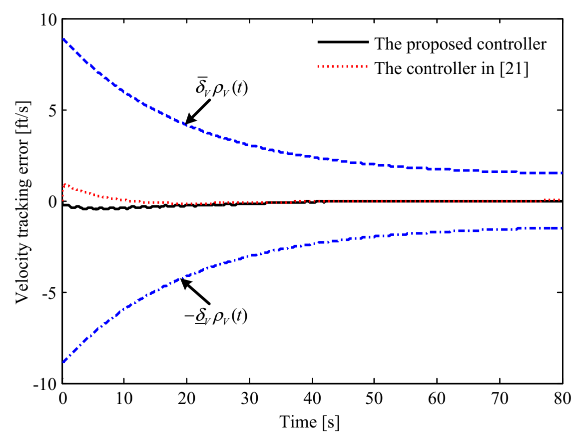

Fig. 3 Velocity tracking error

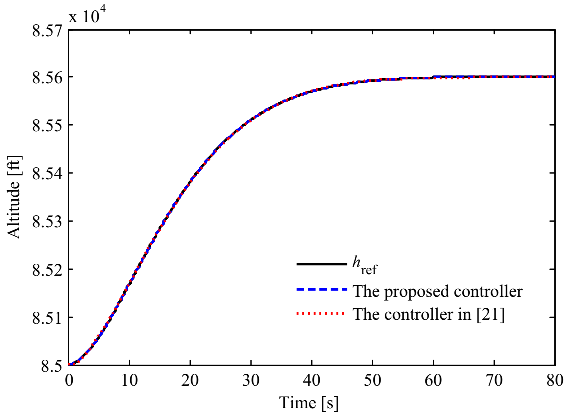

Fig. 4 Altitude tracking performance

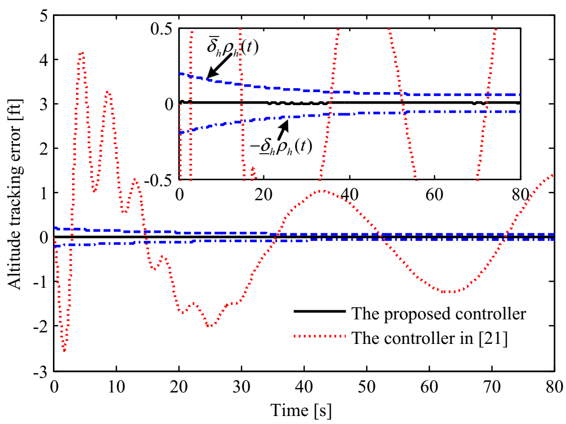

Fig. 5 Altitude tracking error

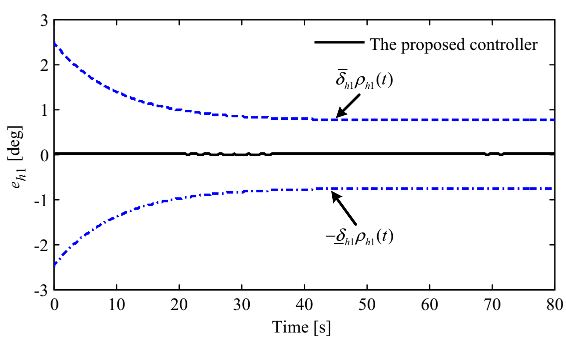

Fig. 6 The response of e_{h1}

$k_{h2} = 0.02$, $\rho_{h30} = 0.087$, $\rho_{h3\infty} = 0.026$, $l_{h3} = 0.1$, $\delta_{h3} = \bar{\delta}_{h3} = 0.5$, $\kappa_{h31} = -40$, $\kappa_{h32} = 0.5$. Moreover, all the model coefficients in (1)–(7) are assumed to be uncertain by defining $C = C_0\,[1 + 0.3\sin(0.05\pi t)]$,

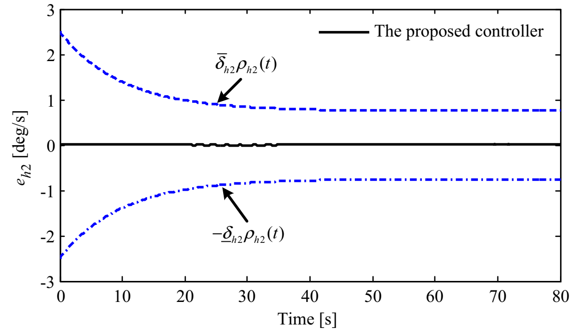

Fig. 7 The response of e_{h2}

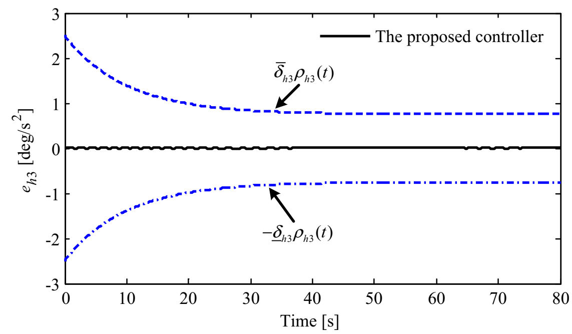

Fig. 8 The response of e_{h3}

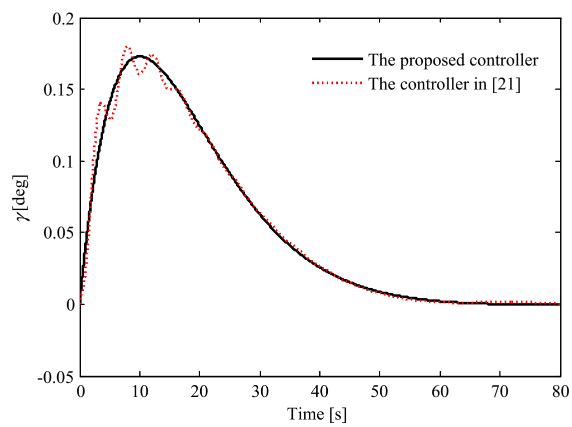

Fig. 9 The response of γ

where C denotes the value of uncertain coefficient and C_0 is the normal value of C.

The tracking performance of the presented control approach is depicted in Figs. 2, 3, 4, 5, 6, 7, 8, 9, 10, 11, 12 and 13. Figures 2, 3, 4, 5, 6, 7 and 8 show that all the tracking errors are forced to fall within prescribed boundaries in the presence of parametric uncertainties. Thus, the pursued control objective is achieved. Fur-

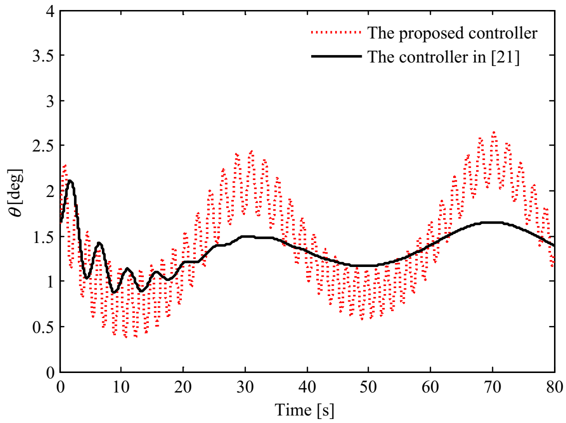

Fig. 10 The response of θ

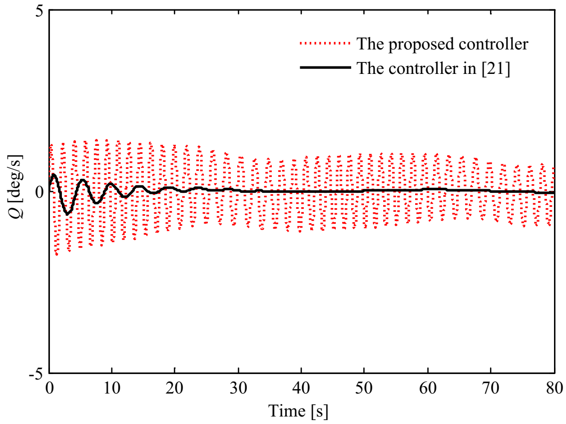

Fig. 11 The response of Q

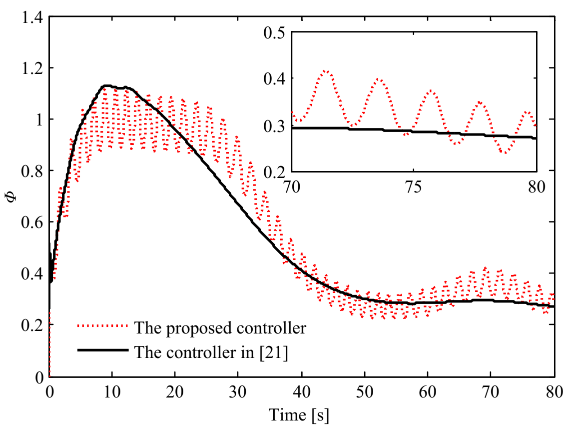

Fig. 12 The control input Φ

ther, it is observed from Figs. 3, 4 and 5 that velocity and altitude tracking error converge to zero faster when using the proposed controllers than by employing

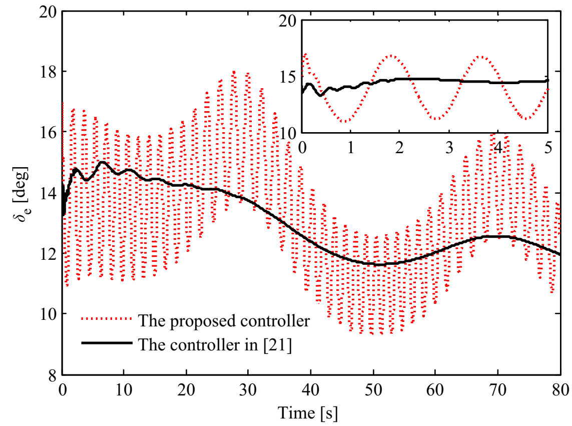

Fig. 13 The control input δ_e

the strategy of [20], which indicates that better transient performance can be provided by the addressed controller than by the one presented in [20]. Besides, the responses of attitude angles and control inputs, as shown in Figs. 9, 10, 11, 12 and 13, reveal that these variables are bounded and vary without high-frequency chattering. To sum up, the addressed control approach can provide robust tracking of velocity and altitude commands with better transient performance in comparison with the control method of [20].

6 Conclusions

In this paper, a prescribed performance controller is exploited for AHVs within the back-stepping framework. The control laws are devised utilizing non-affine models. Prescribed boundaries are constructed by introducing performance functions to constrain tracking errors. Desired transient performance is guaranteed for control systems. The presented control method does not need accurate models or the signs of control gains. Both the robustness and practicality of the controller are fine. The stability of the closed-loop control system is proved via Lyapunov synthesis. Finally, the tracking performance and superiority of the design is validated by numerical simulation results.

Acknowledgements This work was supported by National Natural Science Foundation of China (Grant No. 61603410).

References

1. Wang, J., Zong, Q., Su, R., Tian, B.: Continuous high order sliding mode controller design for a flexible air-breathing hypersonic vehicle. ISA Trans. **53**, 690–698 (2014)

2. Shao, X., Wang, H.: Active disturbance rejection based trajectory linearization control for hypersonic reentry vehicle with bounded uncertainties. ISA Trans. **54**, 27–38 (2015)
3. Xu, B.: Robust adaptive neural control of flexible hypersonic flight vehicle with dead-zone input nonlinearity. Nonlinear Dyn. **80**, 1509–1520 (2015)
4. Bu, X., Wei, D., Wu, X., Huang, J.: Guaranteeing preselected tracking quality for air-breathing hypersonic non-affine models with an unknown control direction via concise neural control. J. Frankl. Inst. **353**, 3207–3232 (2016)
5. Guo, B., Liu, J.: Neural network-based adaptive backstepping control for hypersonic flight vehicles with prescribed tracking performance. Math. Probl. Eng. (2015). https://doi.org/10.1155/2015/591789
6. Bu, X., Wu, X., Huang, J., Wei, D.: A guaranteed transient performance-based adaptive neural control scheme with low-complexity computation for flexible air-breathing hypersonic vehicles. Nonlinear Dyn. **84**, 2175–2194 (2016)
7. Chen, M., Wu, Q., Jiang, C., Jiang, B.: Guaranteed transient performance based control with input saturation for near space vehicles. Sci. China Inf. Sci. **57**(052204), 1–12 (2014)
8. Wilcox, Z., MacKunis, W., Bhat, S., Lind, R., Dixon, W.: Lyapunov-based exponential tracking control of a hypersonic aircraft with aerothermoelastic effects. J. Guid. Control Dyn. **33**(4), 1213–1224 (2010)
9. Preller, D., Smart, M.: Longitudinal control strategy for hypersonic accelerating vehicles. J. Spacecr. Rockets (2015). https://doi.org/10.2514/1.A32934
10. Zhang, Y., Xian, B.: Continuous nonlinear asymptotic tracking control of an air-breathing hypersonic vehicle with flexible structural dynamics and external disturbances. Nonlinear Dyn. **83**, 867–891 (2016)
11. Mu, C., Sun, C., Xu, W.: Fast sliding mode control on air-breathing hypersonic vehicles with transient response analysis. Proc. IMechE Part I: J. Syst. Control Eng. **230**(1), 23–34 (2016)
12. Wu, H., Liu, Z., Guo, L.: Robust L_∞-gain fuzzy disturbance observer-based control design with adaptive bounding for a hypersonic vehicle. IEEE Trans. Fuzzy Syst. **22**(6), 1401–1412 (2014)
13. Zong, Q., Wang, F., Tian, B., Su, R.: Robust adaptive dynamic surface control design for a flexible air-breathing hypersonic vehicle with input constraints and uncertainty. Nonlinear Dyn. **78**, 289–315 (2014)
14. Bu, X., Wu, X., Wei, D., Huang, J.: Neural-approximation-based robust adaptive control of flexible air-breathing hypersonic vehicles with parametric uncertainties and control input constraints. Inf. Sci. **346–347**, 29–43 (2016)
15. An, H., Liu, J., Wang, C., Wu, L.: Approximate back-stepping fault-tolerant control of the flexible air-breathing hypersonic vehicle. IEEE/ASME Trans. Mechatron. **21**(3), 1680–1691 (2016)
16. Wu, G., Meng, X.: Nonlinear disturbance observer based robust backstepping control for a flexible air-breathing hypersonic vehicle. Aerosp. Sci. Technol. **54**, 174–182 (2016)
17. Xu, B., Zhang, Y.: Neural discrete back-stepping control of hypersonic flight vehicle with equivalent prediction model. Neurocomputing **154**, 337–346 (2015)
18. Bu, X., Wu, X., Zhang, R., Ma, Z., Huang, J.: Tracking differentiator design for the robust backstepping control of a flexible air-breathing hypersonic vehicle. J. Frankl. Inst. **352**(4), 1739–1765 (2015)
19. Zhang, Y., Li, R., Xue, T., Lei, Z.: Exponential sliding mode tracking control via back-stepping approach for a hypersonic vehicle with mismatched uncertainty. J. Frankl. Inst. **353**, 2319–2343 (2016)
20. Zhang, S., Li, C., Zhu, J.: Composite dynamic surface control of hypersonic flight dynamics using neural networks. Sci. China Inf. Sci. **58**(070203), 1–9 (2015)
21. Xu, B., Gao, D., Wang, S.: Adaptive neural control based on HGO for hypersonic flight vehicles. Sci. China Inf. Sci. **54**(3), 511–520 (2011)
22. Xu, B., Fan, Y., Zhang, S.: Minimal-learning-parameter technique based adaptive neural control of hypersonic flight dynamics without back-stepping. Neurocomputing **164**, 201–209 (2015)
23. Xu, B., Zhang, Q., Pan, Y.: Neural network based dynamic surface control of hypersonic flight dynamics using small-gain theorem. Neurocomputing **173**, 690–699 (2016)
24. Chen, B., Liu, X., Liu, K., Lin, C.: Direct adaptive fuzzy control of nonlinear strict-feedback systems. Automatica **45**, 1530–1535 (2009)
25. Bolender, M., Doman, D.: Nonlinear longitudinal dynamical model of an air-breathing hypersonic vehicle. J. Spacecr. Rockets **44**, 374–387 (2007)
26. Parker, J., Serrani, A., Yurkonich, S., Bolender, M., Doman, D.: Control-oriented modeling of an air-breathing hypersonic vehicle. J. Guid. Control Dyn. **30**(3), 856–869 (2007)
27. Du, H., Chen, X.: NN-based output feedback adaptive variable structure control for a class of non-affine nonlinear systems: a nonseparation principle design. Neurocomputing **72**, 2009–2016 (2009)
28. Gao, D., Wang, S., Zhang, H.: A singularly perturbed system approach to adaptive neural back-stepping control design of hypersonic vehicles. J. Intell. Robot. Syst. **73**, 249–259 (2014)
29. Ge, S., Hong, F., Lee, T.: Adaptive neural control of nonlinear time-delay systems with unknown virtual control coefficients. IEEE Trans. Syst. Man Cybern. Part B Cybern. **34**(1), 499–516 (2004)